

DEVELOPMENT OF AN INTEGRATED NOZZLE FOR A SYMMETRIC, RBCC LAUNCH VEHICLE CONFIGURATION

2001035060

Timothy D. Smith
National Aeronautics and Space Administration
Glenn Research Center
Cleveland, Ohio

Francisco Canabal III
National Aeronautics and Space Administration
Marshall Space Flight Center
Huntsville, Alabama

Tharen Rice
Johns Hopkins University
Applied Physics Laboratory
Baltimore, Maryland

Bernard Blaha
Ohio Aerospace Institute
Brook Park, Ohio

SUMMARY

The development of rocket based combined cycle (RBCC) engines is highly dependent upon integrating several different modes of operation into a single system. One of the key components to develop acceptable performance levels through each mode of operation is the nozzle. It must be highly integrated to serve the expansion processes of both rocket and air-breathing modes without undue weight, drag, or complexity. The NASA GTX configuration requires a fixed geometry, altitude-compensating nozzle configuration. The initial configuration, used mainly to estimate weight and cooling requirements was a 15° half-angle cone, which cuts a concave surface from a point within the flowpath to the vehicle trailing edge. Results of 3-D CFD calculations on this geometry are presented. To address the critical issues associated with integrated, fixed geometry, multimode nozzle development, the GTX team has initiated a series of tasks to evolve the nozzle design, and validate performance levels. An overview of these tasks is given.

The first element is a design activity to develop tools for integration of efficient expansion surfaces with the existing flowpath and vehicle aft-body, and to develop a second-generation nozzle design. A preliminary result using a "streamline-tracing" technique is presented. As the nozzle design evolves, a combination of 3-D CFD analysis and experimental evaluation will be used to validate the design procedure and determine the installed performance for propulsion cycle modeling. The initial experimental effort will consist of cold-flow experiments designed to validate the general trends of the streamline-tracing methodology and anchor the CFD analysis. Experiments will also be conducted to simulate nozzle performance during each mode of operation. As the design matures, hot-fire tests will be conducted to refine performance estimates and anchor more sophisticated reacting-flow analysis.

BACKGROUND

NASA Glenn Research Center is currently developing propulsion system technologies for a single-stage to orbit (SSTO) rocket based combined cycle (RBCC) vehicle. The GTX (ref. 1) concept vehicle is a vertical take-off reusable SSTO launch vehicle concept. The current engine configuration is based upon a 300-lb payload reference vehicle.

As shown in figure 1, the GTX is an axisymmetric vertical launch vehicle with three engine flowpaths equally spaced 120° apart. Each engine flowpath is an independent RBCC engine that consists of a movable spike inlet, internal rocket, and ramjet/scramjet flowpath (fig. 2). The centerbody of the vehicle is used as the nozzle expansion surface, with the flowpaths converging on a fixed geometry, altitude compensating sculpted aft-body. Further details on the GTX vehicle design and performance metrics can be found in reference 1.

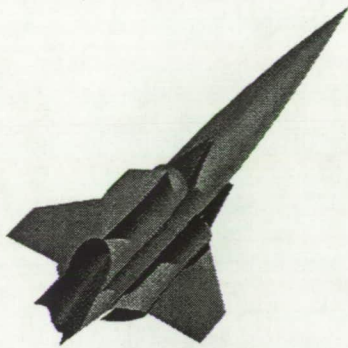


Figure 1.—GTX single-stage-to-orbit rocket based combined cycle vehicle.

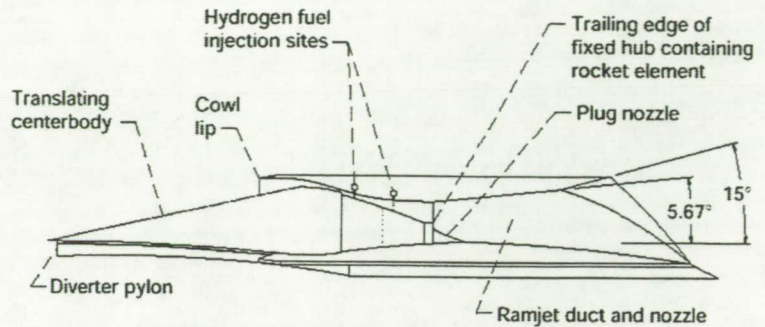


Figure 2.—Schematic of the GTX propulsion flowpath.

The key to any RBCC engine flowpath is the integration of multiple types of operating cycles into a single unique system. The GTX engine will operate in four modes; (1) air-augmented rocket, (2) thermally-choked ramjet, (3) scramjet, and (4) all-rocket. The low-speed system for lift-off through Mach 3 is called the "Independent Ramjet Stream" (IRS) cycle (ref. 2). This system, like most RBCC low-speed systems, is an air-augmented rocket configuration. The rocket is used for lift-off and as the rocket fires; air is entrained through the inlet. However, instead of requiring mixing with the rocket stream, the ram airflow remains independent of the rocket exhaust and is fueled by the upstream ramjet and scramjet injectors. The rocket continues to operate and serves as the pilot for the secondary flow. The result is a mode of operation that is neither an optimized ramjet, nor an optimized rocket. Examining other modes of operation show that there are several areas of compromise in the system. During scramjet operation, the hub that houses the rocket creates a significant backward facing step, which reduces overall performance. During mode 4 ascent-to-orbit (ATO) operation, the rocket is required to fire through the flowpath before expanding on the aft cone, whereas a conventional launch vehicle rocket would be located in the aft of the vehicle with an optimized nozzle for flow expansion. Previous analysis (ref. 3) has shown that the free expansion of the rocket into the flow path and length of the flowpath can have a significant affect on performance. One key thread running through each of the modes is the need for an efficient method to expand the flow and generate the required specific impulse.

FLOWPATH DESCRIPTION

Key aspects to designing an efficient nozzle for hypersonic vehicles are to use the available projected area and provide altitude compensation. The first iterations of the GTX had a simple truncated cone located downstream of the flowpath exit. However, since the propulsion system is not purely annular around the vehicle exit, the gaps between the propulsion pods present potential losses due to spillage. Previous work (ref. 4) has shown that for an annular plug with discrete thruster locations that the spacing between thrusters is an important loss mechanism. As a result, adjustments were required to prevent flow spillage around the pods.

The method selected was to lay in a conical surface with the endpoint located in the flow path and carve out a surface such that each engine pod had a discrete expansion surface, yet still take advantage of the aft-body surface. Figure 3 shows the inlay of a 15° conical expansion into the flowpath as it was cut into the aft body.

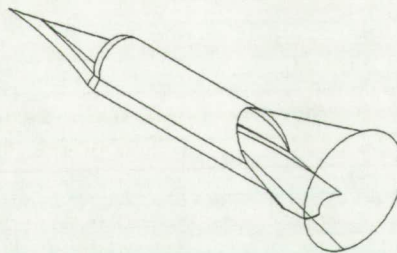


Figure 3.—Baseline flowpath expansion geometry.

This initial configuration provided a starting point for both nozzle performance and flowpath weight assessments. The configuration and contour are sized such that the configuration should not change significantly in terms of weight or structure. However, it has been understood since the beginning that a more robust approach to the nozzle design would be required. The modified aft body cone provides a point of departure for nozzle analysis and evaluation of design evolution.

The most obvious nozzle on the GTX vehicle is the aft-body. Flow areas for each station of the flowpath were obtained via one dimensional cycle analysis. Key area locations are shown in figure 4. Table I provides the key locations in the flow, for a single flowpath, along with the corresponding areas and area ratios.

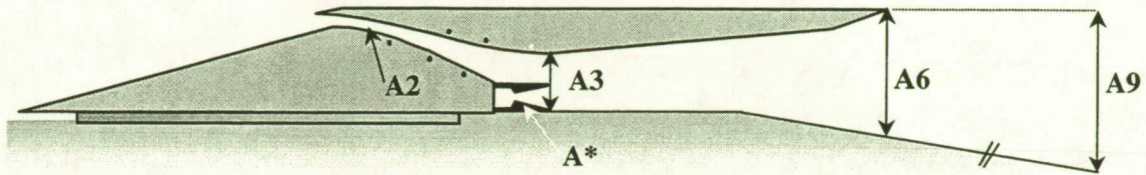


Figure 4.—GTX propulsion pod geometry and area locations.

TABLE I.—GTX ENGINE FLOWPATH AREAS AND AREA RATIOS.

Location		Area, in ²	Area ratio
Rocket throat area	A*	42.8	
Scram combustor throat area	A2	523.5	
Ram combustor throat area	A3	2512.9	
Flowpath exit area	A6	7829.0	
Nozzle exit area	A9	17438.0	
	A9/A*		407.20
	A6/A3		3.12
	A9/A3		6.94

Integration of the rocket into the flowpath also plays a critical role in setting the flow lines. To start with, the nozzle must be packaged to reduce drag and blockage. The rocket nozzle must provide some measure of altitude compensation for both modes 1 and 4. During the mode 1 transition from IRS to pure ramjet operation, the ramjet combustion pressure is higher than the rocket nozzle exit pressure; therefore the nozzle could be susceptible to separation. Mode 4 is also critical because the rocket is firing for nearly half of the trajectory. Unlike conventional rockets that use an optimized bell nozzle, the flow must go through a free expansion before expanding on the aft vehicle surface. Due to the free expansion and low ambient backpressure, a measure of altitude compensation is also required. Two configurations, a semi-axisymmetric plug and scarfed nozzle, are being evaluated to meet the rocket performance requirements. Both are intended to reduce blockage while providing a surface for altitude compensation. The plug nozzle design was used in the CFD analysis, however a subsequent structural design study has shown the plug to be heavier and more difficult to manufacture. Currently, a more detailed study is underway to evaluate integration of scarfed rocket nozzles for GTX.

As discussed previously, the engine must operate over a range of conditions and Mach numbers. Table II presents the operating conditions of the engine through out the trajectory.

TABLE II.—GTX FLOWPATH OPERATING ENVELOPE.

Mach number	Altitude, ft	Combustor total pressure, psia	Nozzle pressure ratio
0	0		
2	27,280	24.3	4.9
2.5	36,952	33.0	10.5
3	44,625	44.0	20.1
4	56,682	80.6	65.9
5	66,055	131.2	167.1
6	79,928	102.3	251.0
8	92,349	165.0	718.0
10	102,000	289.5	1961.7
12	110,000	488.5	4741.5
ATO	150,000+		Inf

The main figure of merit for nozzle performance in the cycle analysis is gross thrust coefficient. The definition used is the experimental thrust normalized by the ideal thrust when expanded to ambient pressure.

$$C_{fg} = \frac{F_{EXP}}{F_{IDEAL}}$$

The target values for GTX nozzle performance are: $C_{fg} = 0.85$ to 0.95 for Mach < 5.5 , $C_{fg} = 0.95$ for Mach 5.5 to 11, and $I_{spv} > 450$ sec for mode 4.

CFD ANALYSIS

A three-dimensional computational fluid dynamics (CFD) analysis was conducted to provide an initial evaluation of nozzle performance over a range of conditions. The analysis (ref. 5) was performed at the NASA Marshall Space Flight Center using the FDNS (ref. 6) code with finite rate chemistry. Turbulence was modeled with a standard $k-\epsilon$ model with wall function. The solutions were used to calculate nozzle thrust, which was normalized by ideal thrust to obtain gross thrust coefficient, C_{fg} . For this analysis, a total of three modes of operation were analyzed with FDNS:

- Mode 1 at Sea Level
- Mode 3 at Mach = 10
- Mode 4 near vacuum conditions

The cases analyzed assume zero angle-of-attack and zero yaw angle, therefore only a 60-degree sector of the vehicle was modeled. This sector lies between the engine flowpath plane of symmetry, and a plane of symmetry between two adjacent propulsion flowpaths. To account for the freestream effects, the domain of the CFD model extends approximately six cowl lip radii from the vehicle axis in the radial direction. In the axial direction, the model extends downstream approximately one length of a propulsion flowpath from the vehicle base and upstream one cowl length from the nozzle exit. Figure 5 shows a representative grid domain.

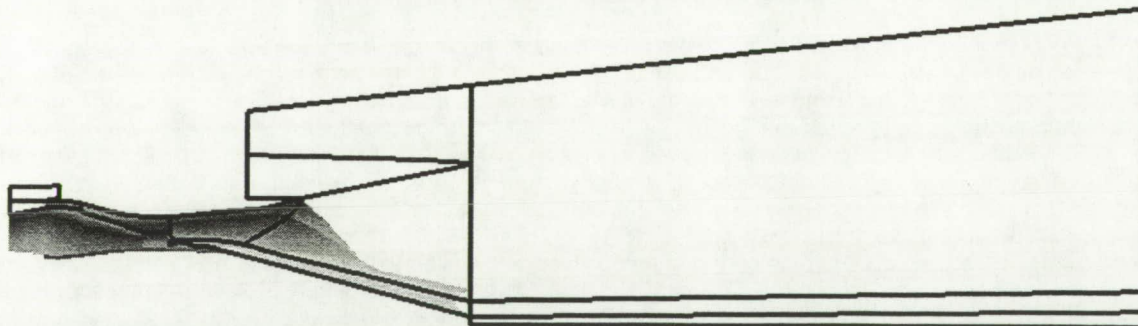


Figure 5.—CFD grid domain for GTX flowpath analysis.

Total thrust was calculated by numerically integrating the axial components of momentum, pressure, and skin friction forces. Gross thrust coefficient was obtained by normalizing the computed thrust by the ideal thrust. The ideal thrust was evaluated by isentropically expanding the one-dimensional conditions to ambient pressure. Ideal thrust is then the product of the velocity and mass flow rate.

Mode 1 at Sea Level.—Mode 1 is the lift-off portion of the trajectory; as a result freestream Mach number was zero for this analysis. At lift-off, the inlet center body is in the full open position, which allows for air to be entrained as the thrusters operate. The rockets are operating at a chamber pressure of 1500-psia and a mixture ratio of 6.0. A one-dimensional chemical analysis code (ref. 7) was used to obtain the flowfield properties at the rocket throat. Both frozen and finite rate chemistry conditions were considered to study the combustion performance.

Figure 6 shows the normalized pressure contour plot for the mode 1 analysis. The large areas of low pressure downstream of the rocket present a significant area of concern for this operation. These areas are caused by the acceleration of the entrained air as it passes through the engine due to the ejector effect produced by the rocket. A related affect is the over expansion of the rocket due to the lower static pressure created by the entrained flow. The

result is a lower than desired thrust coefficient, depending upon frozen or finite rate chemistry assumptions. The frozen thrust coefficient was calculated to be 62.9 percent, while the finite rate solutions produced a thrust coefficient of 64.4 percent. The main difference between the two results is a pressure increase in the finite rate solution due to afterburning.

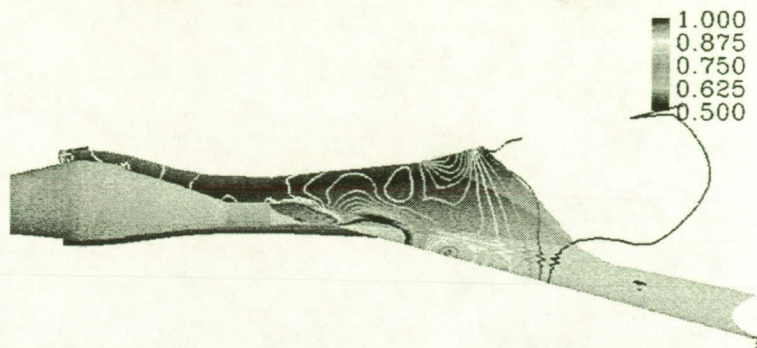


Figure 6.—Pressure contours at symmetry plane (pressure in atm, finite rate chemistry).

Mode 3 at Mach 10.—Mode 3 operation is while the engine is operating in a scramjet configuration. As a result, the inlet is translated near the aft most position. The freestream conditions were based upon a vehicle flying an altitude of 101 800 ft. A one-dimensional analysis was performed to obtain the supersonic flow conditions at the expansion onset plane. The onset plane is the location along the inlet section of the flowpath, downstream of which it is assumed that no further scramjet combustion occurs and the flow begins to expand. This condition corresponded to a flow field equilibrium Mach number of 2.208, a static temperature of 5092 R, and a freestream static pressure ratio of 185.76. The equilibrium conditions for the supersonic combustion of air and hydrogen were obtained for an equivalence ratio of 1 and a combustion efficiency of 95 percent.

Results from this analysis were much more encouraging than the initial mode 1 calculations. Figure 7 presents the pressure contour plots for the scramjet flow. The main area of concern during scramjet operation is the backward facing step in the flow that results from the rocket hub. As shown, this area does present a problem due to the recirculation zone at the rocket hub, which reduces thrust by producing an area of low pressure on the step. A thrust coefficient of 90.7 percent was calculated for frozen flow, while the finite-rate result was slightly higher at 91.3 percent.

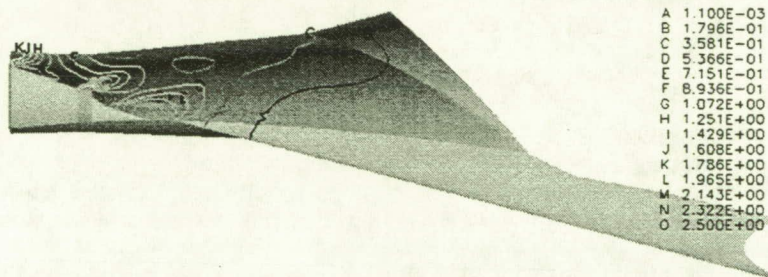


Figure 7.—Pressure contour at the symmetry plane (pressure in atm, finite rate chemistry).

Mode 4 near vacuum conditions.—During mode 4, the rocket is operating without any airflow into the system as the vehicle ascends to orbit through the thinnest sections of the atmosphere. The rockets are operating at a chamber pressure of 1500-psia and a mixture ratio of 6.0. For the CFD simulation, the flowfield properties were obtained at the rocket throat using a one-dimensional chemical analysis code and the chemical composition of the gas was combined into a single equivalent gas assuming frozen chemistry. In this section of the flight trajectory, the inlet is in the full aft closed position, which helps to prevent flow from potentially escaping out the front of the flowpath as the ambient pressure nears vacuum conditions. By closing the inlet, a cavity is now created upstream of the rocket thrusters. This cavity can be a potential loss mechanism as the rockets are firing by creating a low-pressure region due to ejector effects. One method to alleviate this potential loss mechanism is to provide bleed flow in to the cavity and increase the pressure on the aft facing surfaces. Although the bleed can help to reduce the losses associated with the cavity, the optimum amount of bleed must be determined that provides the desired thrust increase without

reducing specific impulse. To examine the bleed effects, a parametric analysis was performed by varying the amount of bleed flow from 0 to 5 percent. Figure 8 presents the Mach number contours for the 5 percent bleed case during mode 4 operation.

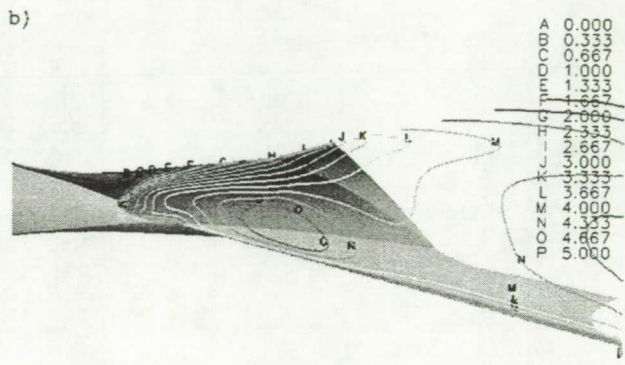


Figure 8.—Mach number contours at the symmetry plane, 5 percent bleed flow.

Two sets of results are important for mode 4 operation, thrust coefficient and specific impulse efficiency. As discussed previously, the amount of secondary bleed flow is an important factor for improving the rocket expansion process. However, an optimum value exists where the benefit to thrust performance does not reduce specific impulse. Table III presents both the specific impulse and thrust coefficient results for a range of bleed flows.

TABLE III.—MODE 4 CFD RESULTS FOR SPECIFIC IMPULSE AND THRUST COEFFICIENT AS A FUNCTION OF BLEED FLOW.

Percent of bleed flow	Isp, sec	C _{1g} , percent
0.0	414.9	85.0
2.5	415.4	86.5
5.0	413.5	87.4

The results provide an interesting situation, in that while thrust coefficient increases with bleed flow, the specific impulse is maximized at 2.5 percent bleed flow.

SECOND GENERATION NOZZLE DESIGN

The baseline GTX nozzle was considered a starting point for performance, structural, and weight analysis. From the beginning, it was recognized that a more directed design effort would be required to meet the target C_{1g} of 0.95. To develop the second-generation nozzle configuration, a grant (ref. 8) has been initiated with The Johns Hopkins University Applied Physics Laboratory to study innovative nozzle configurations. A brief summary of the activities will be presented in the following section.

To meet the objective of designing a high performance nozzle a new tool based on streamline tracing was developed for the design of three-dimensional nozzle shapes. Streamline tracing has been used extensively in the past to develop waverider concepts (refs. 9 to 12). The most recognizable example of the streamline tracing technique is the Busemann inlet. To better understand the application of streamline tracing, some basic definitions and an explanation of the technique are presented.

By definition, for a steady flow, a streamline defines the path of particles whose velocity is tangent to the path at all points. If **V** denotes the velocity vector field and the local vector tangent to the streamline is **ds**, the equation defining the stream shape can be written as:

$$\mathbf{V} \times d\mathbf{s} = 0$$

Furthermore, a boundary defined by multiple streamlines defines a streamtube. Conservation of mass requires that the mass flow be constant within the streamtubes.

Neglecting viscous effects, a wall can be inserted along any portion of a streamtube without modifying the shape characteristics of the streamtube itself. This feature serves as the basis for the design of three-dimensional shapes. By using streamlines from a known flowfield, such as a two-dimensional or conical flow, complex three-dimensional shapes can be traced. Since the streamlines are derived from a known flowfield, all of the flow properties

(i.e., pressure, temperature, velocity) along those streamlines are known for the design condition. The streamline tracing technique assumes that the boundary layer characteristics of the derived three-dimensional design will not significantly alter the inviscid flowfield.

Applying streamline tracing to the design of nozzles presents some slightly different assumptions as compared to inlets or vehicles. Whereas with inlets and vehicles the inflow is considered an infinitely large freestream without a predefined geometry, for the nozzle many inflow factors are already set, in particular the nozzle throat. The key is to then determine the proper baseline flowfield and location of the existing nozzle throat geometry within the flowfield. For the GTX designs, an internally expanding axisymmetric bell nozzle was selected as the basic flowfield for the streamline tracing. One item to note is that there are infinite possibilities, however in an axisymmetric flowfield, the shape of the stream tube at the entrance and exit will be the same except for a basic scale factor corresponding to the nozzle expansion ratio.

To develop the GTX designs, a set of four design tools were used. The Rao nozzle design code (ref. 13) was used to develop the optimum axisymmetric contour given the entrance properties, area ratio, and length-to-throat radius ratio. The Two-Dimensional Kinetics (TDK97) (ref. 14) program was then used to generate the method of characteristics (MOC) grid, where the pressure, temperature, velocity, and flow angle are known at each grid point. Nozzle streamlines were then generated using the Streamline Tracing Tool (STT), which was developed specifically for this task. STT starts at the nozzle entrance plane and mines the MOC grid data to determine the streamlines. For a given streamline, the mass flow between that streamline and an adjacent streamline is constant. STT finds the MOC grid point where the mass flow remains constant. With the streamlines known, the solution is imported into a computer aided design program (ref. 15) where the flowfield is contoured based upon the flowpath shape to create the final geometry.

The design methodology described in the previous section was used to develop a new nozzle geometry for the GTX flowpath. Several constraints were placed on the design based upon performance and weight goals. The constraints were:

- Limit on the length of the body-side nozzle
- Limit on the length of the cowl-side nozzle
- Maximum surface of the cowl less than the maximum surface area of the cowl with the 15° cone design.
- Area at the cowl exit plane greater than 1.25 times the combustor entrance area at Mach 2 freestream conditions.
- No increase in projected area, nozzle must be in the shadow of body/nacelle cross-section.

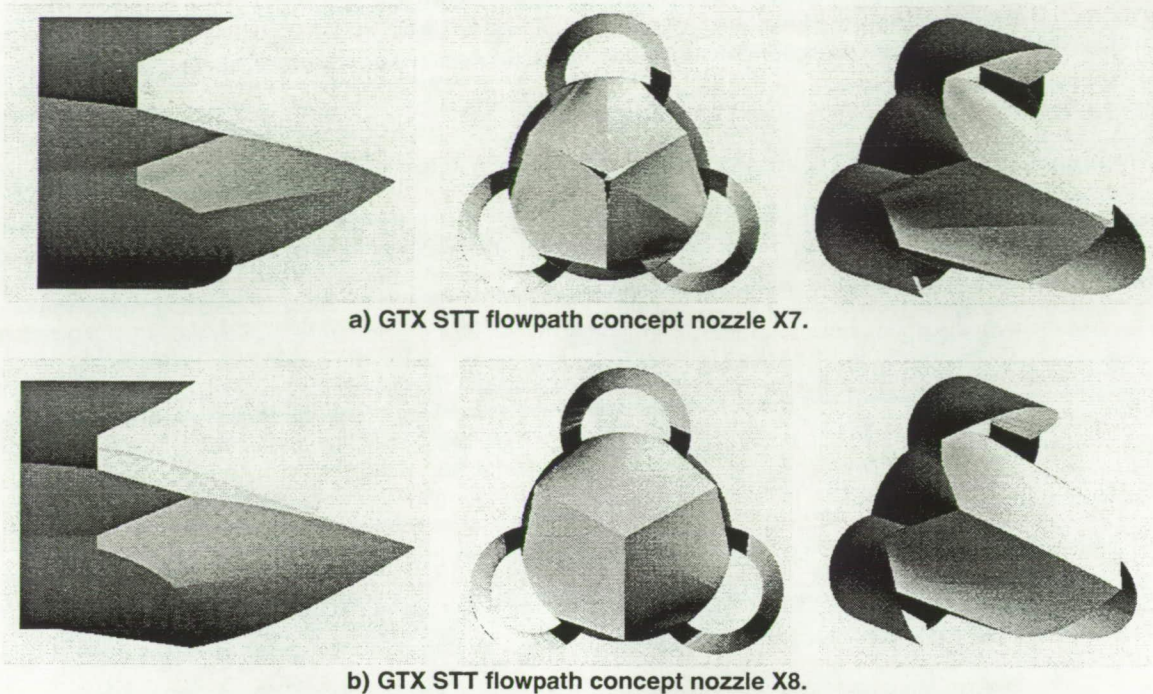
Based upon the constraints, the most appropriate throat geometry orientation with respect to the streamline flow was determined. Other critical factors that were evaluated as part of the design process include body and cowl-side divergence losses and cowl-side length. The axisymmetric nozzle solutions were then used to determine the nozzle shape that met each of the constraints.

For the initial analysis, the nozzle inflow plane started at the point downstream of the hub where the body-side divergence was initiated. The flow properties were determined from a one-dimensional isentropic calculation where the combustor exit conditions corresponded to Mach 8 conditions. A simplifying assumption was no losses between the end of the scram combustor and the nozzle start. This neglects the expected dump losses from the hub and any losses due to friction forces. Table IV summarizes the flow properties at the nozzle inflow plane.

**TABLE IV.—MACH 8 FLOW PROPERTIES
BASED UPON 1-D ANALYSIS.**

	Combustor exit	Nozzle entrance
Pressure, psia	54.2	10.0
Temperature, R	4924	3897
Velocity, ft/s	5862	8052
Mach	1.71	2.61
γ	1.25	1.25

Using the design methodology described, two nozzle solutions (X7 and X8) were obtained. Figures 9(a) and (b) show designs X7 and X8, respectively. The designs were based on different area ratios for the starting optimum nozzle design. Nozzle design X7 is based on an area ratio of 49, while design X8 is based on an area ratio of 64. One of the most obvious features of the new nozzle designs is the convex shape of the body-side nozzle surface. Another unique feature to the design are the notched cowl side surfaces, which were added to increase the nozzle exit area at station 6.



a) GTX STT flowpath concept nozzle X7.

b) GTX STT flowpath concept nozzle X8.

Figure 9.—Streamline traced aft-body configurations. a) design X7 b) nozzle X8.

Pressure contour plots were used to calculate thrust coefficient. The calculated C_{Tg} for nozzle designs X7 and X8 were 92.7 and 91.9 percent respectively. To better understand the loss mechanisms, C_{Tg} was broken down into four components

$$C_{Tg} = 1 - \Delta C_{TgDivergence} - \Delta C_{TgFriction} - \Delta C_{TgKinetics} - \Delta C_{TgUnderExpansion}$$

Performance results are summarized in table V.

TABLE V.—THRUST COEFFICIENT AND LOSS MECHANISM BREAK DOWN FOR STREAMTUBE BASED NOZZLE DESIGNS.

	X7	X8
C_{Tg}	92.7	91.9
$\Delta C_{TgDivergence}$	4.7	5.6
$\Delta C_{TgFriction}$	0.6	0.6
$\Delta C_{TgKinetics}$	0.3	0.3
$\Delta C_{TgUnderExpansion}$	1.7	1.7
Gross thrust, lbf	231467	229449

Both nozzle designs are lower than the target value of 95 percent for thrust coefficient. The most obvious loss mechanism for these designs is divergence, nearly double all other losses combined. This suggests that additional emphasis needs to be placed on exit angle affects. Future designs will also need to expand the design space and possibly relax some of the constraints placed upon the design space. Finally, more in-depth analysis with at 3-D CFD code will be required before a final determination can be made regarding any streamtube design.

EXPERIMENTAL PROGRAM

To go along with the analytical efforts for a nozzle design, an experimental program is being formulated to test multiple nozzle configurations. The test effort will result in multiple test rig development that will feed into an integrated engine test platform. Because of the unique nature of the flowpath it is critical to validate the numerical results by building hardware and performing experimental tests. It is planned that many of the tests will be conducted in par-

allel with the CFD and design activities. The test rigs will take an evolutionary approach to flowpath nozzle development by building an information base with small-scale rigs before eventually moving into integrated flowpath tests. Several key objectives must be met with the experiments to refine the GTX flowpath:

- Develop mission optimized nozzle contours and integration
- Validate nozzle performance during mode operations
- Anchor 3-D CFD analysis

One of the significant challenges facing an experimental program for RBCC applications is finding facilities that can test over a wide range of conditions. This problem is heightened for nozzle components due to the wide range of pressure ratios and flow conditions required. To test the full flowpath over the full range of conditions requires a facility that must be able to provide high pressure internal flows to simulate combustion components while providing ambient back pressures down to vacuum conditions.

Subscale Static Testing.—The initial series of test being developed will be to examine the flowpath over a range of simulated conditions. The test hardware will be a subscale version of the flowpath from station 3 to station 9. Multiple hardware configurations will be evaluated based upon the results from the CFD analysis and the streamline tracing design tasks. Tests will be conducted at a range of test conditions from Mach 3 to ATO. Rig flow will be into a static pressure environment that simulates ambient pressure the altitude corresponding to each Mach number. Heated air will be used as the working fluid. Temperatures will be elevated to levels sufficient to prevent condensation in the exhaust. The goal of the activity will be to conduct parametric tests to compare relative performance levels for streamline traced nozzle designs against the current baseline GTX design. Sufficient static pressure measurements will be collected for comparison with and validation of the CFD predictions. The main figure of merit for these experiments will be C_{I_9} values based on measured thrust.

A second test rig is being developed to specifically look at how the scramjet flowpath will affect nozzle performance. The main concern with the scramjet flow is the backward facing step of the rocket hub. The sudden expansion in the flow will certainly result in performance degradation, however the exact levels are unknown. Also unknown is if any special design changes can be made to alleviate some of the losses due to the step in the flow. The throat will simulate station 2 in the GTX flow path, with the hardware duplicating the annular flowpath past the inlet cowl. As with the general flow rig, heated air will be used as the working fluid, which will be flowing into a static pressure environment. Pressure and thrust measurements will be used to benchmark against the CFD analysis and determine overall performance levels.

One of the more interesting series of tests planned will be to examine the GTX flowpath during mode 4 or ATO operations. For this experiment a simulated rocket thruster will be used inside of the flow path. The goal of the experiments will be to examine the effect on performance of the rocket free expansion. Unlike a conventional rocket, which utilizes an optimized bell nozzle, the flowpath for the rocket in ATO has the potential for significant losses due to the non-optimal shape. A second goal of the experiment will be to introduce secondary flow into a cavity upstream of the rocket hub to see if there is any improvement in performance. One of the keys to this experiment will be the ability to test at high area ratios with a near vacuum environment. This will provide a cost effective means for evaluation of ATO performance without requiring hot-fire experiments in large rocket vacuum facilities. This set of experiments is critical to providing data on a portion of the RBCC flight trajectory that is not well understood, yet has a dramatic affect on performance.

Wind Tunnel Testing.—A follow on to the static testing will be a series of wind tunnel tests to evaluate freestream affects on nozzle performance. Previous experiments (ref. 16) have shown that the ambient flowfield around the vehicle can interact with the external exhaust flow, thus changing the results that were expected based on static conditions. Testing would be conducted from Mach 0.4 to 3.5, with special focus around transonic conditions.

The propulsion pod would be integrated into an isolated axisymmetric nacelle model, with faired over inlets. The axisymmetric nacelle provides clean, uniform flow for the valid development and evaluation of isolated nozzle performance. The model is ~8.5-in. in diameter, which was selected to be compatible with classic transonic wind tunnel testing blockage criteria; <1 percent of the tunnel flow for Mach numbers near 1.0, yet large enough for appropriate Reynolds numbers. Test fluids will be supplied by two separate high-pressure fluid systems, one to supply the simulated rocket, and one to supply the air-breathing flowpath. The support systems would float on a bearing system to allow the axial motion needed for accurate force measurement. The external surface of the cylindrical nacelle upstream of a "metric break station" and the wind tunnel support strut would all be grounded. All of the scale nozzle external and internal components aft of the metric break station will be supported on the bearing system with the air supplies. The system will be grounded through a single load-cell capable of both thrust and drag force measurement.

Integrated Flowpath Testing.—The ground test development of the GTX flowpath will be pulled together into a series of integrated systems tests. The series of test articles will develop and demonstrate the integration of flowpath components, flight-type materials and structures, engine systems, controls and thermal management. The final build will serve as a prototype and test engine for the sub-scale, sub-orbital GTX flight demonstration vehicle. Integrating the results from the nozzle CFD and experimental efforts will be a critical aspect to success of the demonstration testing.

The initial experiments will be with hardware made from boilerplate construction with water-cooling. Propellants will be pressure-fed to reduce operational complexity. Testing will be focused primarily on the air-breathing modes of operation. The goal will be to keep the hardware to a sufficient scale, which allows testing over the widest possible Mach range. Continued development will lead to a more flight-like prototype engine. Boilerplate hardware will be replaced by components made from advanced materials to demonstrate flight weight application. Focus of the testing will shift to engine demonstration, specifically thermal management and cycle performance. A key series of tests will be conducted in vacuum conditions to evaluate the nozzle design during mode 4 operation.

SUMMARY

The nozzle development for the GTX RBCC propulsion system concept is a critical component for the success of this highly integrated system. The nozzle must be adaptable to operate in four distinct modes over a range of Mach numbers. The nozzle must also be integrated into the GTX vehicle to provide maximum expansion area without significant increases in weight, drag, or structural requirements. A fixed geometry, altitude-compensating aft-body has been selected as the baseline nozzle.

Initial analysis has been conducted on a baseline geometry using 3-D CFD for three modes of operations. The main figure of merit for the analysis was nozzle thrust coefficient, target C_{T_0} is 95 percent for each mode of operation. Results from the sea level static analysis show a significant drop in performance due to air entrainment from the rocket. Nominal C_{T_0} values ranged between 62.9 to 64.4 percent. Analysis of mode 3 at Mach 10 showed a significant increase in performance, with a nominal C_{T_0} of 91 percent. The final operation analyzed was the ascent to orbit mode where the rockets are the sole propulsion system operating. Due to greater than desired divergence losses, nozzle C_{T_0} ranged from 85.0 to 87.4 percent.

To address the identified gaps in nozzle performance, a task is underway to develop the second-generation nozzle designs. The method is based on a streamline tracing technique that has been used previously for inlet and vehicle designs. The goal of the activity is to develop highly 3-D nozzle designs based upon the unique shape of the RBCC flowpath. The streamline tracing technique allows for the design of a complex shape to be based on the ideal flow stream of optimized bell type nozzles.

Finally, a series of experimental test rigs are under development to evaluate the new designs in both cold-flow and hot-fire tests. The results will be used to refine and update the streamline tracing design code, along with benchmarking CFD results. The combination of sub-scale experimental rig data and CFD results will provide the stepping-stones to critical integrated systems testing.

REFERENCES

1. Trefny, C.J.: "An Air-Breathing Launch Vehicle Concept for Single-Stage-To-Orbit" AIAA-99-2730, June 1999.
2. Yungster, S. and Trefny, C.J.: "Analysis of a New Rocket-Based-Combined-Cycle Engine Concept at Low Speed," AIAA-99-2393, June 1999.
3. Smith, T.D., Steffen, C.J., Yungster, S., and Keller, D.J.: Performance of an Axisymmetric Rocket Based Combined Cycle Engine During Rocket. NASA TM-206639.
4. Unconventional Nozzle Tradeoff Study. Aerojet Liquid Rocket Company. Contract NAS3-20109, N79-28224, July 1979.
5. Canabal III, F.: Evaluation of the Trailblazer Nozzle Performance. Internal NASA Memorandum. March 2000.
6. Chen, Y.S.: FDNS-A General Purpose CFD Code, Version 4.0. Engineering Sciences, Inc., ESI-TR-97-01, Huntsville, AL May 1997.
7. Gordon, S. and McBride, B.J.: Computer Program for Calculation of Complex Chemical Equilibrium Compositions and Applications. NASA RP-1311, 1994.
8. Rice, T. and Van Wie, D.M.: Design of Exhaust Nozzle for the RBCC-Trailblazer Concept-Final Report. The Johns Hopkins University-Applied Physics Laboratory, AATDL-00-033. NAS3-99146. February 2000.
9. Van Wie, D.M. and Molder, S.: Applications of Busemann Inlet Designs for Flight at Hypersonic Speeds. AIAA 92-1210, February 1992.
10. Nonweiler, T.R.F.: Delta Wings of Shapes Amenable to Exact Shock-Wave Theory. Journal of the Royal Aeronautical Society, Vol. 67, 1963.
11. Maikaper, G.I.: Bodies Formed by the Stream Surfaces of Conical Flows. Fluid Dynamics, Vol. 1, No. 1, 1966.
12. Rasmussen, M.L.: Waverider Configurations Derived from Inclined Circular and Elliptic Cones. Journal of Spacecraft and Rockets, Vol. 17, Nov.-Dec. 1980.
13. Nickerson, G.: The RAO Method Optimum Nozzle Contour Program Users Manual. Software and Engineering Associates, Inc., June 1995.
14. Nickerson, G., et al.: TDK97, Two-Dimensional Kinetics (TDK) Nozzle Performance Computer Program Users Manual, Software and Engineering Associates, Inc., January 1998.
15. ICEM CFD 4.0: Users Manual, ICEM CFD Engineering, Berkeley, CA, January 2000.
16. Trefny, C.J., DeBonis, J.C., Shyne, R.J., and Lam, D.W.: Results of a Single-Expansion-Ramp Nozzle Experiment With Hot Exhaust and External Burning. NASA TM-106390.